



能谱CT在肺部磨玻璃结节良恶性鉴别中的应用价值

安冬会,杨俊潇,屈亚林,谢慧,吴绍全

重庆医科大学附属第一医院大足医院/重庆市大足区人民医院放射科,重庆 402360

【摘要】目的:探讨肺混合性磨玻璃结节能谱计算机断层扫描成像(CT)特异性征象,通过对各种结节成分和征象的分析对肺微浸润癌(MIA)、浸润性腺癌(IPA)及肺结核腺泡结节(AN)进行鉴别诊断。**方法:**回顾性分析156例肺混合磨玻璃结节及肺结核腺泡结节患者的能谱CT扫描图像及临床资料,并结合病理结果进行对比讨论。**结果:**156例患者共有221个结节,均经过手术及送病理检查,包括62个MIA、76个IPA、78个AN、3个硬化性血管瘤及2个炎性假瘤。其中,MIA组结节CT值较低,约为(-221±101)HU,其征象主要为空泡征,占45.16%;IPA组CT值较MIA组高,约为(-102±54)HU,主要征象为分叶征,占47.36%;AN组CT值最高,约为(-40±27)HU,CT征象结节边缘平滑,占70.51%。3组病例CT值及CT征象存在统计学差异($P<0.05$)。**结论:**能谱CT形态学特征能在一定程度上鉴别MIA、IPA及AN,为临床早期诊疗不同疾病提供相关依据。

【关键词】肺疾病;混合磨玻璃结节;肺结核;计算机断层扫描成像

【中图分类号】R445.3

【文献标志码】A

【文章编号】1005-202X(2018)10-1160-04

Application value of energy spectrum CT in the differential diagnosis of benign and malignant pulmonary ground-glass nodule

AN Donghui, YANG Junxiao, QU Yalin, XIE Hui, WU Shaoquan

Department of Radiology, the Dazu District People's Hospital/Dazu Hospital of the First Affiliated Hospital of Chongqing Medical University, Chongqing 402360, China

Abstract: Objective To investigate the specific signs of energy spectrum computed tomography (CT) of pulmonary mixed ground-glass nodules, and to perform a differential diagnosis of minimally invasive adenocarcinoma (MIA), invasive pulmonary adenocarcinoma (IPA) and alveolar nodules (AN) based on the components of nodules and CT signs. **Methods** The CT scan images and clinical date of 156 patients with pulmonary mixed ground-glass nodules and AN were retrospectively analyzed and compared with the pathological results. **Results** A total of 221 nodules were found in 156 patients. All patients underwent surgery and pathological examination. The nodules include 62 MIA, 76 IPA, 78 AN, 3 sclerosing hemangioma and 2 inflammatory pseudotumor. The CT value of the nodules was found to be the highest in AN group, about (-40±27) HU, followed by IPA group and then MIA group, about (-102±54) and (-221±101) HU, respectively. The main CT sign in MIA, IPA, and AN groups was vacuoles (45.16%), lobulated (47.36%), and smooth margin (70.51%), respectively. Statistical differences were found in CT values and CT signs among the 3 groups ($P<0.05$). **Conclusion** The morphological feature of energy spectrum CT can identify MIA, IPA and AN, providing relevant evidences to the differential diagnosis and treatment.

Keywords: lung disease; mixed ground-glass nodule; tuberculosis; computed tomography

前言

近年来,随着影像技术的发展,肺部小结节的检出率越来越高,肺混合性磨玻璃结节作为一种主要

【收稿日期】2018-04-28

【基金项目】重庆市卫生计生委医学科研项目(2017MSXM180)

【作者简介】安冬会,主治医师,主要从事影像诊断,擅长各种疾病的诊断和介入治疗,E-mail: dvfs212@126.com

【通信作者】杨俊潇,主治医师,主要从事放射医学影像诊断,E-mail: fenghuo58@163.com

的表现形式,存在于肺部病变中,而引起混合性磨玻璃结节的主要原因为肺腺癌^[1]。2011年国际多学科学会对肺腺癌制定了新的病理分类标准^[2],该标准取消了“细支气管肺泡癌”,引入“肺微浸润癌(Minimally Invasive Adenocarcinoma, MIA)”,认为对于肺部1 cm左右的磨玻璃结节除了原位腺癌(Adenocarcinoma *in situ*, AIS)外,还存在MIA和浸润性腺癌(Invasive Pulmonary Adenocarcinoma, IPA)的可能。有研究报导AIS和MIA早期切除后,其5年无瘤生存率接近100%^[3],但IPA的预后情况较差,且肺

腺癌的女性发病率高于男性^[4]。在初治性肺结核中的肺腺泡结节CT表现多为混合性磨玻璃结节,在临床症状不典型时容易误诊,因此探讨这3种不同性质结节的典型CT形态学征象,对临床诊断具有重要的指导意义。

1 资料与方法

1.1 临床资料

回顾性分析重庆医科大学附属第一医院大足医院2012年6月至2017年8月收治的156例行能谱CT扫描及手术病理证实患者共221个混合性磨玻璃结节的CT征象表现(大小、边界、密度、空泡征、分叶征)及临床资料(性别、临床症状及病理结果)。其中男性68例,年龄20~87岁,中位年龄49岁;女性88例,年龄22~79岁,中位年龄52岁。89例出现咳嗽、咳痰、发热、胸痛等临床症状,其中初治肺结核患者56例,占62.9%;67例无临床症状,体检时发现病灶遂入院进一步检查。行手术切除后病理证实221个结节,包括62个MIA(28.054%)、76个IPA(34.389%)、78个肺结核腺泡结节(AN)(35.294%)、3个硬化性血管瘤(1.357%)及2个炎性假瘤(0.905%)。

1.2 检查方法及图像处理

所有病人都采用GE宝石能谱CT(Discovery CT750 HD,美国)进行检查,检查前叮嘱病人做好相关准备,用能谱扫描模式行平扫,范围为双侧肺尖到膈面。扫描

参数:自动管电流,管电压为80~140 kV,层厚、间隔均为5 mm,探测器宽度64.000×0.625 mm。原始图像重建采用的层厚及层间距为0.625 mm,传至AW 4.3工作站,应用多平面重组技术,分别在不同层面上进行3次测量,取平均值,其中,磨玻璃结节取实性成分密度。由两位高年资放射科主治医师在工作站上对影像征象进行分析,包括结节边缘、空泡征及分叶征。当两者意见不一时,由副主任医师组织科室集体读片讨论,得出统一结论。

1.3 统计学方法

采用SPSS 19.0软件进行统计学分析,计数资料以%表示,计量资料以均数±标准差表示,采用 χ^2 检验,以 $P<0.05$ 表示差异有统计学意义。

2 结 果

MIA组及IPA组磨玻璃结节直径较AN组大,MIA组较IPA组小;MIA及IPA组实性成分密度较AN组低,MIA明显低于IPA组;在病灶内部,空泡征的出现率MIA及IPA均显著高于AN组,且MIA与IPA组间存在统计学差异($P<0.05$)。在病灶边缘,AN组边界光滑,呈圆形或椭圆形,较MIA及IPA组差异明显,有统计学意义($P<0.008$),而MIA及IPA组间比较差异无统计学意义。分叶征出现率以IPA组最高,与MIA组间比较差异有统计学意义($P<0.05$)。详见图1及表1。

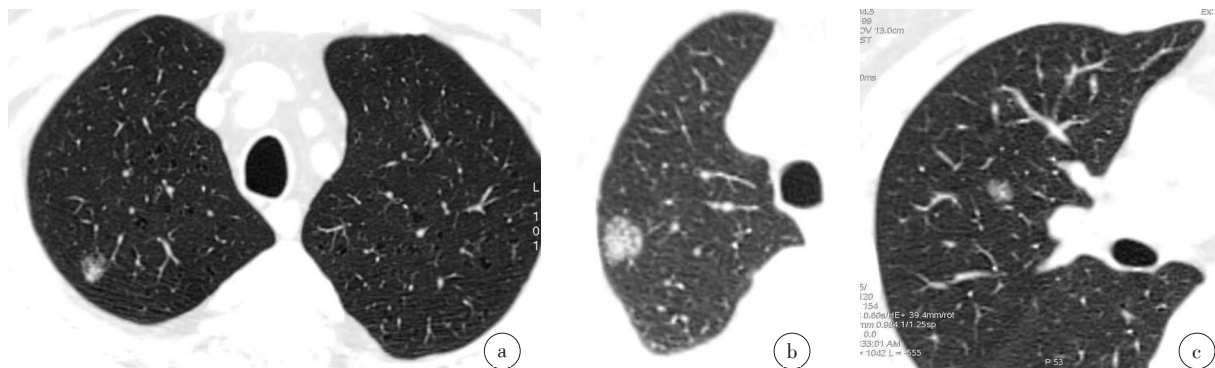


图1 肺部3种类型磨玻璃结节影
Fig.1 Images of 3 types of pulmonary ground-glass nodules

Fig.1a was the image of 61 years old male diagnosed with AIS, with a ground-glass nodule in the posterior segment of the right upper lobe, in which vacuole signs were observed; Fig.1b was the image of 43 years old male diagnosed with MIA, and a mixed ground-glass nodule was observed at the tip of the right upper lobe, with a lobulated sign; Fig.1c was the image of 38 years old female diagnosed with tuberculosis, and an acinar nodule was observed at the anterior segment of the right upper lobe, similar to ground-glass density, with smooth margin.

3 讨 论

3.1 磨玻璃结节的病理生理机制及对应CT特征

磨玻璃结节是指肺内部局限性的密度增高影,

因其密度不能掩盖末梢支气管血管束,形似磨砂玻璃样而得名^[5]。其病理生理机制为:肺组织在正常健康状态时,吸气肺泡腔扩张,吸入空气,呼气肺泡壁



表1 MIA、IPA 及 AN 组 CT 典型征象比较
Tab.1 Comparison of CT features among MIA, IPA and AN groups

CT sign	MIA group (<i>n</i> =62)	IPA group (<i>n</i> =76)	AN group (<i>n</i> =78)	<i>P</i> value
Diameter/mm	11.8±1.2 ^a	18.5±7.1	9.4±0.7	<0.050
Density/HU	-221±101 ^a	-102±54	-40±27	<0.050
Vacuole	28(45.16%) ^a	31(40.78%)	14(17.94%)	<0.008
Smooth margin	16(25.81%)	9(11.84%)	55(70.51%) ^b	<0.008
Lobulated	18(29.03%)	36(47.36%) ^b	9(11.53%)	<0.050

MIA: Minimally invasive adenocarcinoma; IPA: Invasive pulmonary adenocarcinoma; AN: Alveolar nodules; Compared with IPA group, ^a*P*<0.05; Compared with MIA group, ^b*P*<0.05

弹性回缩,气体进行血氧交换,一旦人体肺部处于非健康状态,肺泡腔不能扩张,残气不能排出,其内残留液体,当出现炎性及肿瘤性浸润时,肺泡组织局部密度增加,肺泡单位体积气体减少,单位像素气体变少,遂CT扫描肺组织密度增加,显示为磨玻璃结节。大多磨玻璃结节边缘光滑,吴芳等^[6]提出1 cm以下边缘光滑的磨玻璃结节中,存在AIS较多;Lee等^[7]提出可以用磨玻璃结节的横断面最大径来鉴别侵袭性病变和侵袭前病变,对于纯磨玻璃结节,两者鉴别最佳直径为10 mm,而对于混合性磨玻璃结节,其临界最大截面为14 mm,本研究中的IPA组平均直径大于这个范围。病灶越大其恶性程度越高^[8],有研究表明IPA内部浸润灶>5 mm,也以实性结节为主,可以表现为磨玻璃结节^[9]。胸部影像学国际学术组织费莱舍尔学会(the Fleischner Society)^[10]要求在CT研究肺混合性结节时,实性成分需>6 mm,实性结节需≥8 mm。最新研究发现在CT引导下穿刺活检的肺小结节中,磨玻璃结节直径>6 mm或≤8 mm,最趋于稳定,恶变机率低^[11]。MIA和IPA的病理机制主要由Clara细胞或Ⅱ型肺泡上皮细胞内肿瘤组织沿肺泡壁及支气管生长,出现浸润或形成堆积,MIA一般是沿肺泡壁伏壁生长,随着肿瘤细胞浸润的进展,加上细胞分化程度及生长速度等的影响,MIA的形态各异,边界不规则。在MIA组,肿瘤性肺泡腔内脱落细胞增多,局部空气含量减少,CT表现空泡征,强烈提示磨玻璃结节为恶性^[12]。进一步发展到IPA时,肿瘤组织侵犯到小支气管及血管,邻近小叶间隔伴纤维组织增生,CT表现上出现分叶征^[13]。胸膜牵拉可出现在MIA中,并具有鉴别诊断意义^[14]。肺结核腺泡结节出现的病理基础是小支气管周围的气腔实变,腺泡腔内主要为渗出性炎变,混合空气像素上表现为磨玻璃密度影^[15],但炎性物质并不侵犯肺泡壁及血管,所以AN组边界多为清晰,很少出现分叶征,内部偶见空泡征,多为肺泡

内的残留气腔所致,当炎症进一步发展为肺小叶性实变,与支气管相通后,易出现空洞。

3.2 宝石能谱CT的低剂量扫描和高质量图像分辨率

低剂量CT由Naidich等^[16]在1990年首次提出,原则是在不降低图像质量的前提下,尽量将辐射剂量降至最低,使人体受到的辐射损害最小。目前,肺部低剂量CT已广泛应用于临床,剂量降低的主要方式是降低管电流,但这样会影响图像的信噪比。图像噪声增加会引起密度分辨率降低,对肺内细微结构(肺小叶、亚段支气管及纵隔结构等)的识别力下降。宝石能谱CT以宝石为探测器材料,其稳定性较传统CT的陶瓷探测器和钨酸镧探测器高出20倍,宝石能谱CT可以保证更好的图像质量和更低的辐射剂量^[17]。能谱成像能实现单光子成像与物质分离,通过X线球管的高低双能瞬时切换以获取高分辨率单能图像^[18],其扫描出的图像具有较高的分辨率。能谱CT图像对肺结节征象显示更清晰,诊断准确率更高^[19]。本研究病例一律采用能谱方式扫描,以0.625 mm层厚及层间隔重建,更清晰地表现出病灶的形态,测量值更为准确。

4 结 论

使用宝石能谱CT对肺部混合性磨玻璃结节和肺结核腺泡结节进行扫描检查能实现低剂量扫描,得到高分辨的CT图像,从而更好地鉴别结节的良恶性程度,有助于患者早期选择手术或对症治疗,提高生存率及生活质量。本研究的局限性在于样本量较小,因大多数肺部小结节病人多选择随访观察,未选择手术,所以病例收集不多;其次,未做增强扫描对比分析,多发结节未单独讨论;再者,由于肺部小结节在影像学特征上存在同病异影和异病同影征象,其良恶性形态学特征可能存在重叠现象^[20],存在一些误差。





【参考文献】

- [1] HARO A, YANO T, KOHNO M, et al. Ground-glass opacity lesions on computed tomography during postoperative surveillance for primary non-small cell lung cancer[J]. Lung Cancer, 2012, 76(1): 56-60.
- [2] TRAVIS W D, BRAMBILLA E, NOGUCHI M, et al. International Association for the Study of Lung Cancer/American Thoracic Society/European Respiratory Society international multidisciplinary classification of lung adenocarcinoma[J]. J Thorac Oncol, 2011, 6(2): 244-285.
- [3] 孙珊珊, 李惠民, 虞峻歲, 等. 肺原位腺癌的超高分辨率CT表现[J]. 中国医学计算机成像杂志, 2016, 22(2): 121-125.
- SUN S S, LI H M, YU L W, et al. CT findings of lung adenocarcinoma *in situ* in ultra-high-resolution computed tomography[J]. Chinese Computed Medical Imaging, 2016, 22(2): 121-125.
- [4] SASADA S, MIYATA Y, TSUBOKAWA N A, et al. Role of positron emission tomography/computed tomography findings for adjuvant chemotherapy indications in stage T1b-2aN0M0 lung adenocarcinoma [J]. Ann Thorac Surg, 2014, 98(2): 417-423.
- [5] 姜明, 刘廷斌. 肺局灶性磨玻璃密度结节的多层次螺旋CT诊断[J]. 系统医学, 2017, 2(2): 91-93.
- JIANG M, LIU Y B. Multislice spiral CT diagnosis of focal nodular nodules in the lung[J]. Systems Medicine, 2017, 2(2): 91-93.
- [6] 吴芳, 蔡祖龙, 田树平, 等. 1 cm以下磨玻璃密度肺腺癌的CT征象与病理亚型及免疫组织化学的相关性[J]. 中国医学科学院学报, 2015, 37(2): 163-170.
- WU F, CAI Z L, TIAN S P, et al. Correlations between pathologic subtypes/immunohistochemical implication and CT characteristics of lung adenocarcinoma ≤ 1 cm with ground-glass opacity[J]. Acta Academiae Medicinae Sinicae, 2015, 37(2): 163-170.
- [7] LEE S M, PARK C M, GOO J M, et al. Invasive pulmonary adenocarcinomas versus preinvasive lesions appearing as ground-glass nodules: differentiation by using CT features[J]. Radiology, 2013, 268 (1): 265-273.
- [8] FAN L, LIU S Y, LI Q C, et al. Multidetector CT features of pulmonary focal ground-glass opacity: differences between benign and malignant [J]. Br J Radiol, 2012, 85(115): 897-904.
- [9] AUSTIN J H, GARG K, ABERLE D, et al. Radiologic implications of the 2011 classification of adenocarcinoma of the lung [J]. Radiology, 2013, 266(1): 62-71.
- [10] MACMAHON H, NAIDICH D P, GOO J M, et al. Guidelines for management of incidental pulmonary nodules detected on CT images: from the Fleischner Society 2017[J]. Radiology, 2017, 284(1): 228-243.
- [11] CHANG Y Y, CHEN C K, YEH Y C, et al. Diagnostic feasibility and safety of CT-guided core biopsy for lung nodules less than or equal to 8 mm: a single-institution experience[J]. Eur Radiol, 2017, 28(2): 796-806.
- [12] 潘峰, 刘卓, 袁飞, 等. 肺局限性磨玻璃结节的高分辨率CT征象与国际肺癌研究协会/美国胸科学会/欧洲呼吸学会病理的对照研究[J]. 中国医学影像学杂志, 2014, 22(11): 815-819, 823.
- PAN F, LIU Z, YUAN F, et al. Comparative study of focal pulmonary ground glass nodule between findings of high resolution CT and pathology classification of IASLC/ATS/ERS[J]. Chinese Journal of Medical Imaging, 2014, 22(11): 815-819, 823.
- [13] 严金岗, 张善华, 王善军, 等. 肺原位腺癌与微浸润腺癌实性成分鉴别诊断[J]. 医学影像学杂志, 2016, 26(11): 2002-2004.
- YAN J G, ZHANG S H, WANG S J, et al. The differential diagnosis of the real components of the adenocarcinoma *in situ* and minimally invasive adenocarcinoma[J]. Journal of Medical Imaging, 2016, 26 (11): 2002-2004.
- [14] 孟庆成, 贾丙鑫, 张建伟, 等. 微浸润型肺腺癌的高分辨率CT表现[J]. 中国医学影像学杂志, 2013, 21(7): 536-538, 542.
- MENG Q C, JIA B X, ZHANG J W, et al. High-resolution CT manifestation of minimally invasive pulmonary adenocarcinoma[J]. Chinese Journal of Medical Imaging, 2013, 21(7): 536-538, 542.
- [15] 谢汝明, 吕岩, 周震, 等. 33例肺结核不典型CT征象分析[J]. 中国防痨杂志, 2014, 36(3): 171-175.
- XIE R M, LÜ Y, ZHOU Z, et al. Characteristic analysis of atypical HRCT findings in 33 patients with pulmonary tuberculosis [J]. Chinese Journal of Antituberculosis, 2014, 36(3): 171-175.
- [16] NAIDICH D P, MARSHALL C H, GRIBBIN C, et al. Low-dose CT of the lungs: preliminary observations[J]. Radiology, 1990, 175(3): 729-731.
- [17] 胡兴和. 宝石能谱CT在早期肺癌筛查中的应用价值[J]. 医疗卫生装备, 2011, 32(12): 64-65, 78.
- HU X H. Application value of gem energy spectrum CT for screening of early lung cancer[J]. Chinese Medical Equipment Journal, 2011, 32(12): 64-65, 78.
- [18] 张芮. 孤立性肺结节的能谱CT分析与形态学研究[D]. 郑州: 郑州大学, 2014.
- ZHANG R. Spectral analysis and morphological characteristics in the differentiation of solitary pulmonary nodules: preliminary study [D]. Zhengzhou: Zhengzhou University, 2014.
- [19] 郭剑波, 李玉林. 能谱CT成像在孤立性肺结节(SPN)良恶性鉴别诊断中的价值及运用[J]. 现代医用影像学, 2016, 25(6): 1052-1054.
- GUO J B, LI Y L. Value of energy spectrum CT in the differential diagnosis of benign and malignant SPN [J]. Modern Medical Imagelogy, 2016, 25(6): 1052-1054.
- [20] 孙凯, 王新文, 张建伟, 等. CT能谱成像对孤立性肺结节鉴别诊断的初步研究[J]. 中国药物与临床, 2015, 15(6): 794-796.
- SUN K, WANG X W, ZHANG J W, et al. The energy spectrum CT imaging's preliminary study to the differential diagnosis of solitary pulmonary nodule[J]. Chinese Remedies & Clinics, 2015, 15(6): 794-796.

(编辑:谭斯允)